Journal of Magnetic Resonance 283 (2017) 110–116

Contents lists available at ScienceDirect

Journal of Magnetic Resonance

journal homepage: www.elsevier.com/locate/jmr

Measurement of backbone hydrogen-deuterium exchange in the type III secretion system needle protein PrgI by solid-state NMR

Veniamin Chevelkov [a], Karin Giller [b], Stefan Becker [b], Adam Lange [a,c,*]

[a] Department of Molecular Biophysics, Leibniz-Forschungsinstitut für Molekulare Pharmakologie, 13125 Berlin, Germany
[b] Department of NMR-Based Structural Biology, Max Planck Institute for Biophysical Chemistry, 37077 Göttingen, Germany
[c] Institut für Biologie, Humboldt-Universität zu Berlin, 10115 Berlin, Germany

ARTICLE INFO

Article history:
Received 9 June 2017
Revised 15 August 2017
Accepted 27 August 2017
Available online 1 September 2017

Keywords:
Magic-angle spinning solid-state NMR
Relax-EXSY
H/D exchange
Deuteration
Amide protons
Proton detection
PrgI
Relaxation

ABSTRACT

In this report we present site-specific measurements of amide hydrogen-deuterium exchange rates in a protein in the solid state phase by MAS NMR. Employing perdeuteration, proton detection and a high external magnetic field we could adopt the highly efficient Relax-EXSY protocol previously developed for liquid state NMR. According to this method, we measured the contribution of hydrogen exchange on apparent ^{15}N longitudinal relaxation rates in samples with differing D_2O buffer content. Differences in the apparent T_1 times allowed us to derive exchange rates for multiple residues in the type III secretion system needle protein.

1. Introduction

Hydrogen exchange provides important information on the structure and dynamics of proteins. In structured protein regions, amide protons are locked into hydrogen bonds and may be solvent-obstructed, which makes hydrogen exchange significantly slower in comparison to amide sites located in unstructured, solvent-exposed regions. Local and/or cooperative protein motion can open hydrogen bonds, and protons can be exchanged. Linderstrøm-Lang introduced a two-step kinetic model to describe this process [1].

Numerous NMR methods have been developed to map exchange rates, which span over several orders of magnitude [2]. Exchange rates in the timeframe of minutes to months can be obtained by monitoring the amide proton signal decay of lyophilized protein dissolved in D_2O buffer [3]. Modifications to this approach allow the monitoring of faster exchange processes [4,5].

To access even faster exchange rates, which are also very important for protein characterization, a variety of pulse sequences have been introduced. Cross peaks between water and amides can be monitored in 3D homonuclear EXchange SpectroscopY experiments (EXSY) [6,7], which require longer measurement time compared to 2D experiments. Saturation transfer techniques allow the use of 2D HSQC experiments to monitor variation in amide magnetization during the hydrogen exchange period defined by a proper experimental scheme [8–12]. However, a number of experimental drawbacks decrease the accuracy of these approaches (see detailed discussion in [13]), in particular amide magnetization evolution due to dipolar couplings with HA, water and hydroxyl protons, and water radiation damping. Recent developments [13–15] aimed to minimize these unwanted effects.

Water-protein interactions in the solid state phase are of great interest, because many proteins are insoluble. Water also plays an important role in the functionality of many biomolecules (e.g. membrane proteins like proton pumps, water channels and ion channels), and solid state NMR (ssNMR) can investigate these processes close to the *in vivo* physiological state. Hydrogen exchange is an important aspect of water-protein interactions and requires accurate quantification.

A previously developed solution state "non-equilibrium" approach [3] was modified for ssNMR studies: hydrogen-deuterium (H/D) exchange between a protonated protein and D_2O buffer is allowed for a certain period of time and amide protonation levels are measured to provide exchange rates [16–21]. The

* Corresponding author at: Department of Molecular Biophysics, Leibniz-Forschungsinstitut für Molekulare Pharmakologie, 13125 Berlin, Germany.
E-mail address: alange@fmp-berlin.de (A. Lange).

https://doi.org/10.1016/j.jmr.2017.08.012
1090-7807/

time required for sample handling defines the slowest possible observable exchange time, which is expected to be on the order of seconds. On the other hand, equilibrium techniques based on saturation transfer can access faster processes and avoid complicated sample handling. However, many of these experiments suffer from alternative magnetization transfer pathways due to proton-proton dipolar interactions. Although in solution state these can safely be ignored in many cases, numerous studies of water-protein interactions in ssNMR demonstrate an extremely short magnetization exchange time on the order of 1 ms between amide protons and water or other protons in the protein, due to strong homonuclear dipolar couplings [22–30]. Even in highly deuterated proteins at fast MAS rates, magnetization exchange times between water and amide protons are 20–100 ms [31,32]. Very often, the hydrogen exchange time is significantly longer and methods that completely eliminate the drawbacks mentioned above are required. One such method is SOLEXSY, which was employed by Reif and coworkers to quantify protein backbone hydrogen exchange in the microcrystalline α-spectrin SH3 domain using the deuterium isotope effect on the amide nitrogen chemical shift to monitor inter-conversion between proton- and deuterium-bound ^{15}N nuclei in H_2O/D_2O buffer [33]. These experiments identified hydrogen exchange for only three amide hydrogens.

Recently, Lippens and coworkers presented Relaxation based EXchange SpectroscopY (Relax-EXSY): a simple and sensitive method [15] to obtain exchange rates for amide hydrogens in solution state. In this approach, the contribution of H/D exchange on the apparent ^{15}N longitudinal relaxation rates measured in buffers containing different D_2O fractions can be used to extract hydrogen exchange rates.

In the present study we employ the Relax-EXSY protocol to obtain site-specific backbone hydrogen exchange rates by solid state MAS NMR in an insoluble, non-crystalline biological assembly, the *Salmonella typhimurium* type III secretion system (T3SS) needle. The supramolecular assembly is formed from the 80 amino-acid protein PrgI. Longitudinal relaxation rates measured for two samples in buffers containing 20% and 100% H_2O fractions are significantly different because of the contribution of H/D exchange, which can be easily extracted. This method demonstrates high sensitivity and is free from drawbacks associated with extraneous magnetization flows, which are typical for saturation transfer schemes.

2. Materials and methods

Two samples were used in the experiments:

(1) fully protonated, uniformly ^{15}N-, sparsely ^{13}C-labeled PrgI protein in 100% H_2O buffer, hereafter referred "protonated",
(2) perdeuterated, uniformly ^{15}N- and ^{13}C-labeled PrgI protein at 20% re-protonation level on labile sites, hereafter referred "deuterated".

Expression, purification and polymerization of wild-type PrgI needles were performed as described previously [34–36]. Isotope labeling in the protonated sample was achieved using $^{15}NH_4Cl$ as the sole nitrogen source and D-[2-^{13}C]-glucose as the sole carbon source during expression [34]. Approximately 25 mg of protonated PrgI was packed into a 3.2 mm rotor.

Isotope labeling in the deuterated sample was achieved using $^{15}NH_4Cl$ as the sole nitrogen source and D-[U-^{13}C, ^{2}H]-glucose as the sole carbon source during expression in D_2O media [36]. The sample was back protonated on labile sites in 20% H_2O buffer [37]. Approximately 25 mg of deuterated PrgI was packed into a 3.2 mm rotor.

2.1. Solid-state NMR spectroscopy

Solid-state NMR experiments for both samples were conducted on an 800 MHz (^1H Larmor frequency) spectrometer (Bruker Biospin, Germany) equipped with a triple-resonance (^1H, ^{13}C, ^{15}N) 3.2 mm probe. Both samples were spun at 20 kHz. The effective sample temperature was measured by the temperature-dependent water proton resonance relative to an internal DSS reference [27]. Chemical shift referencing was done using the internal DSS signal.

Longitudinal relaxation times in the protonated sample were measured employing the pulse sequence introduced earlier [38], using ^{15}N-^{13}CA 2D correlations to obtain residue-specific information (Fig. 1A). Twelve spectra were recorded with corresponding ^{15}N relaxation delays, ΔT, of 0, 5, 9, 17.5, 0, 33, 0, 60, 0, 110, 110 and 0 s. Spectra with 0 s relaxation delay were uniformly distributed over the series for referencing and to normalize peak intensity in adjacent spectra with non-zero delays. All spectra were recorded with 64 scans, except for the two spectra with 110 s relaxation delays, which were recorded with 16 scans. The duration of the initial H-N cross-polarization (CP) transfer [39] was 1.2 ms and the applied average proton and nitrogen RF fields were 78 and 58 kHz, respectively. SPECIFIC CP [40] lasting 3.5 ms was applied for N-CA magnetization transfer. Average ^{15}N and ^{13}C RF fields were 6 and 14 kHz, respectively. During CP transfer, the ^{15}N RF field was ramped from the maximum power down to 80% or from 80% power up to the maximum, as indicated in Fig. 1A. Continuous wave irradiation with a field strength of 76 kHz was applied on the ^1H channel during N-CA magnetization transfer. ^{13}C and ^{15}N maximum acquisition times were 22 ms and 14 ms,

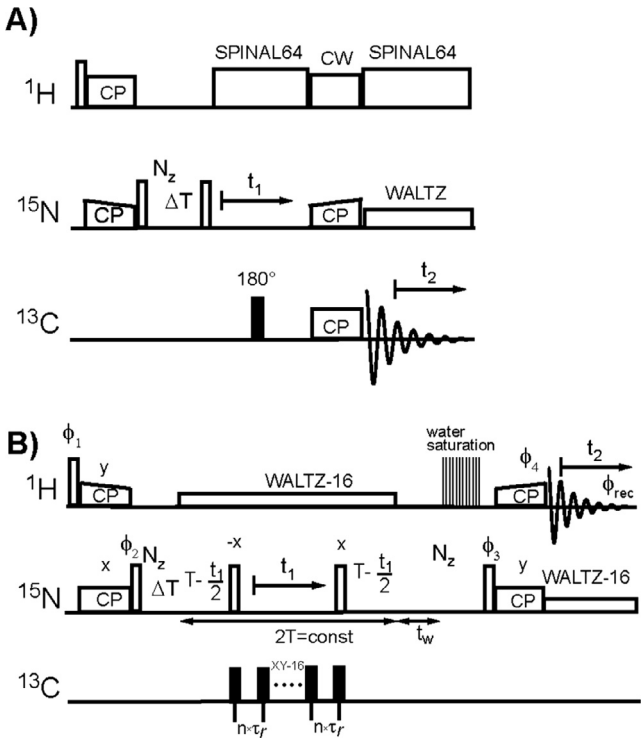

Fig. 1. Pulse sequences employed for the measurement of ^{15}N-T_1 decay rates in the protonated protein (A) and in the extensively deuterated protein (B). Open and filled bars represent 90° and 180° pulses, respectively. Relaxation delays are denoted by ΔT. N_z indicates alignment of ^{15}N polarization along the external field. In panel B, the constant time delay T was set to 60 ms and the phase cycle was ϕ_1 = {x, −x}, ϕ_2 = {y,y, −y, −y}, ϕ_3 = 8 × {y}, 8 × {−y}, ϕ_4 = 16 × {x}, 16 × {−x}, ϕ_{rec} = {x, −x, −x,x, −x,x,x, −x, −x,x,x, −x,x, −x, −x,x}. All other notation follows common rules. The measurements were conducted on an 800 MHz spectrometer at an MAS rate of 20 kHz.

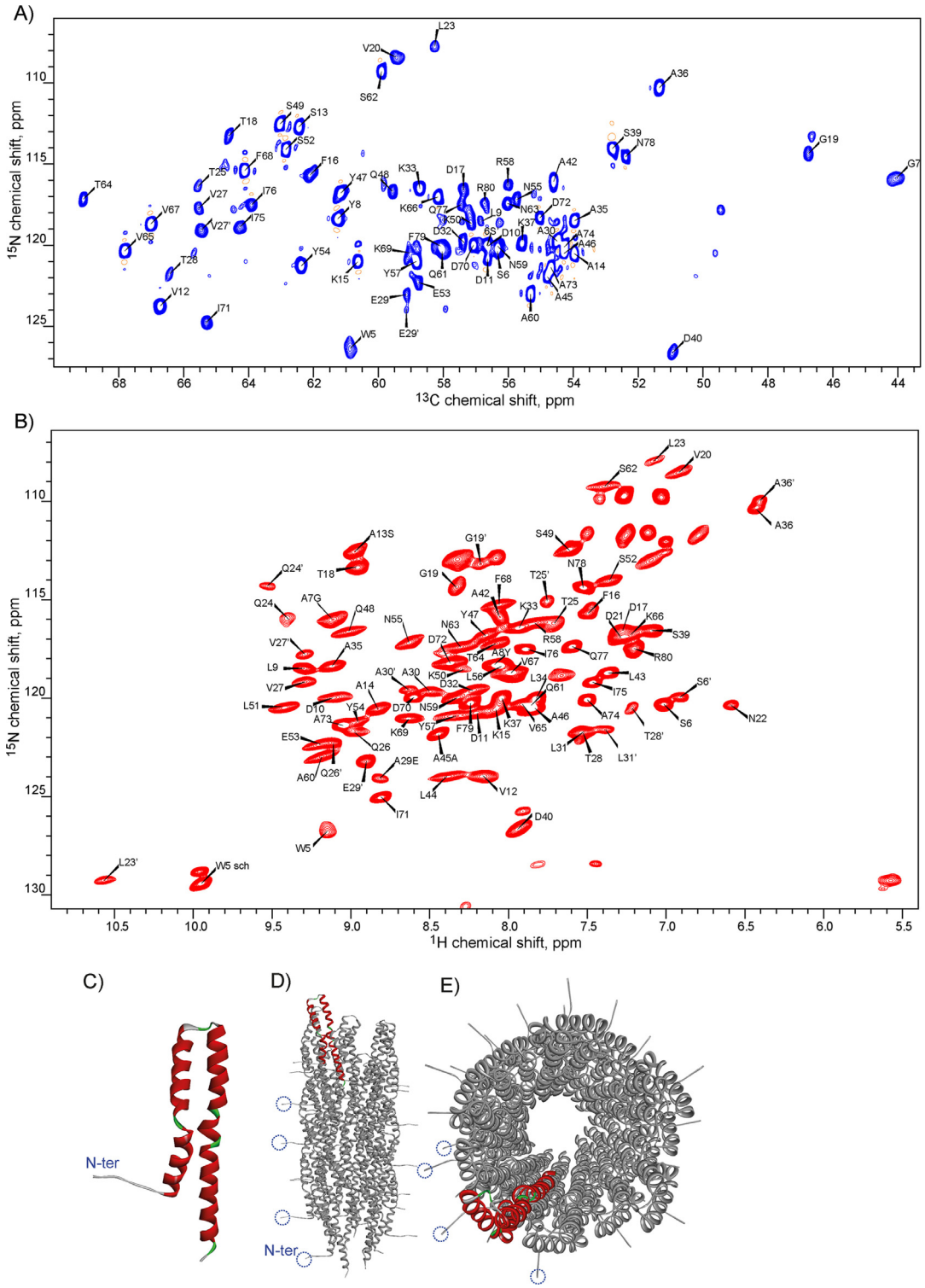

Fig. 2. Two-dimensional carbon-detected (H)NCA (panel A) and proton-detected (H)NH (panel B) correlation spectra of protonated and deuterated PrgI T3SS needles, respectively. The spectra were obtained on an 800 MHz spectrometer at an MAS rate of 20 kHz. The prime sign refers to signals from a second polymorph. Prior to Fourier-transformation the data in the NCA spectrum were apodized with 5 Hz of Lorential broadening in both dimensions, while the data in the HN experiment were apodized with a 60° and 72°-shifted squared sine bell window function for the proton and nitrogen dimensions, respectively. Panel C represents the structure of the single PrgI protein. Side and top views of the T3SS needle are shown in the panel D and E, respectively. Blue dashed circles mark the N-terminus. (For interpretation of the references to color in this figure legend, the reader is referred to the web version of this article.)

respectively. During direct and indirect chemical shift evolution periods, SPINAL-64 [41] heteronuclear decoupling was applied on the ^{1}H channel with an RF strength of 78 kHz. WALTZ-16 [42] with an RF field strength of 2.5 kHz was applied on the ^{15}N channel during ^{13}C detection to remove heteronuclear scalar couplings. During ^{15}N indirect evolution, a hard 180° ^{13}C pulse was used to suppress scalar couplings. The temperature of the protonated sample was set to 4 ± 3 °C.

Fig. 1B represents the pulse sequence for longitudinal relaxation measurements in the deuterated protein, adapted from previous

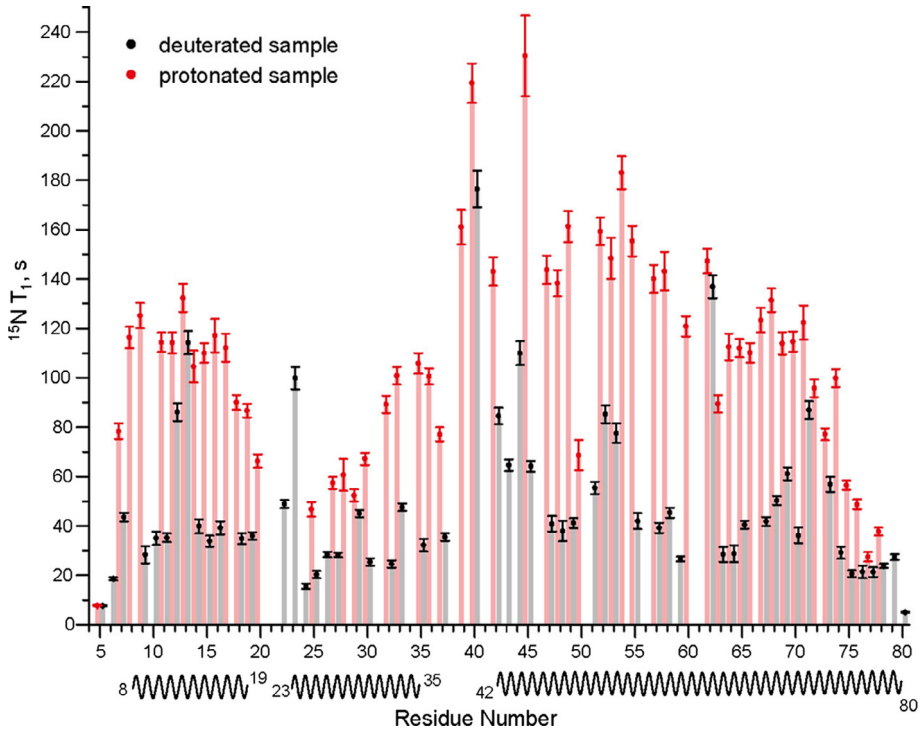

Fig. 3. ^{15}N apparent T$_1$ relaxation times along the primary sequence of PrgI T3SS needles. Results obtained on protonated and deuterated protein presented in red and black, respectively. Secondary structure elements are schematically depicted at the bottom. See Supporting Information (Table 1) for all numeric values. (For interpretation of the references to color in this figure legend, the reader is referred to the web version of this article.)

work [43]. Proton-detected ^{1}H-^{15}N 2D correlations were used to access site-specific relaxation data. Fourteen spectra were recorded with corresponding ^{15}N relaxation delays ΔT of 0, 4.5, 2, 0, 1, 7.5, 15, 0, 42, 0, 25, 0, 25, 0 s. All spectra were recorded with 16 scans.

The initial ^{1}H-^{15}N CP transfer time was set to 1.1 ms, while ^{15}N-^{1}H back transfer was set to 0.38 ms. Average ^{15}N and ^{1}H RF fields were 51 and 71 kHz, respectively. During CP steps the proton RF field was ramped from the maximum power down to 80% or from 80% power up to the maximum, as indicated in Fig. 1B. Both ^{1}H and ^{15}N maximum acquisition times were 40 ms, but during processing ^{1}H FIDs were truncated to 23 ms. During ^{15}N evolution, HN J-couplings were removed by a WALTZ-16 scheme applied on the ^{1}H channel with an RF strength of 3.5 kHz, and NC scalar couplings were suppressed by a train of ^{13}C hard 180° pulses with phase cycling according to the XY-16 scheme and 2 ms interpulse delays. During proton detection, WALTZ-16 with an RF field strength of 3.5 kHz was applied on the ^{15}N channel to remove scalar couplings. Constant time experimental design [44] and MISSISSIPPI [31] were used to minimize the water artefact. The temperature of the deuterated sample was set to 8.5 ± 2 °C.

3. Results and discussion

In order to quantify hydrogen exchange in a solid protein sample at equilibrium conditions, we followed the Relax-EXSY concept previously introduced in liquid state NMR by Lippens and coworkers [15]. Differences between apparent ^{15}N T$_1$ relaxation rates measured in solvents with different D_2O fraction allow for the direct calculation of hydrogen-deuterium substitution rates. Practically, one has to measure apparent ^{15}N longitudinal relaxation rates for two or more samples with different buffer D_2O contents. The protocol was applied to the *Salmonella typhimurium* T3SS needle. Identical 80-residue subunits make a right-handed helical assembly in form of a tube with ~ 80 Å outer diameter and 25 Å lumen diameter. The structure of the single monomer and the top and side view of the assembly are represented in Fig. 2. In the experiment depicted in Fig. 1B, initial amide proton magnetization is transferred to directly bound ^{15}N by CP, while deuterium-bound nitrogens are considered not to be polarized. During the delay ΔT, ^{15}N magnetization aligned along the external magnetic field relaxes to its equilibrium due to protein motion. At the same time, amide protons bound to polarized nitrogens might be substituted by deuterons. After the subsequent NH CP step, magnetization of these nuclei is not observable with proton detection. This effect results in a decrease of the apparent T$_1$. Differences between the apparent T$_1$ obtained in this experiment and the real T$_1$ allow us to calculate the exchange rate. Real relaxation rates can be measured by employing the same experimental scheme for proteins in 100% H_2O buffer or via a carbon detected experiment, which is depicted in Fig. 1A. In the latter experiment, the hydrogen exchange does not influence observed T$_1$ at all and a sample with any buffer D_2O content can be used. In our measurements, real T$_1$ values were obtained on a fully protonated sample by the carbon detected experiment depicted in Fig. 1A.

The employed labeling schemes yield highly resolved and highly sensitive 2D HN and NCA correlations, depicted in Fig. 2. T$_1$ relaxation measurements conducted according to the pulse sequences presented in Fig. 1 show considerable variation in the apparent relaxation rates between protonated and deuterated samples, a consequence of the H/D exchange contribution. Protonated PrgI has a very long T$_1$ [45], which significantly exceeds values obtained on small microcrystalline proteins [38,43,46]. This can be explained by the extremely high rigidity of the T3SS needles. One can see well-pronounced site-to-site variations as well: T$_1$ becomes shorter in the termini and between residues 25 and 35. The apparent T$_1$ for the deuterated sample is considerably shorter, but in general reproduces the overall relaxation profile of

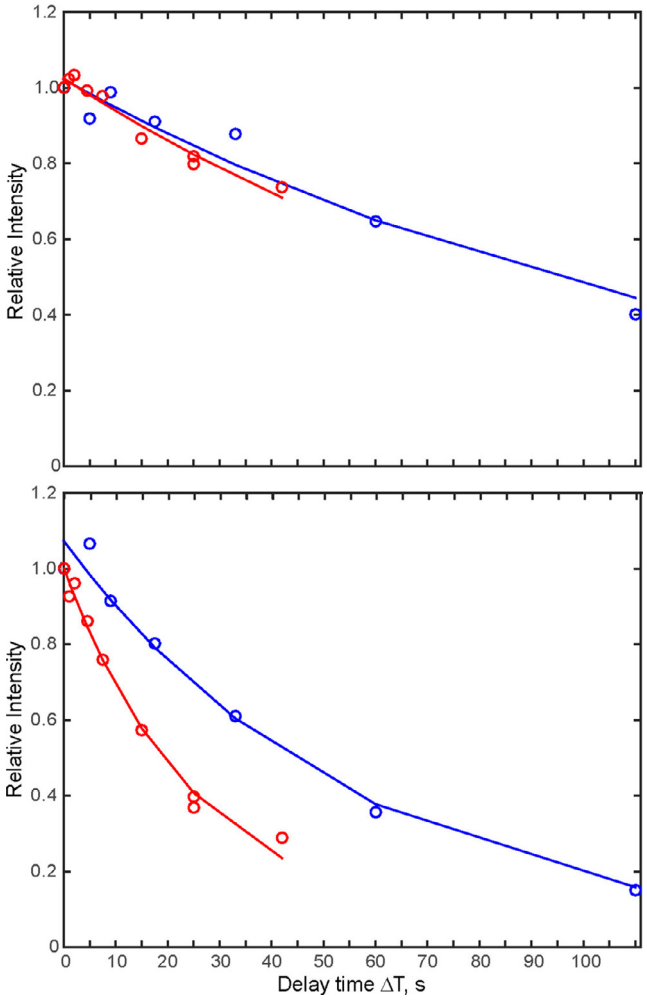

Fig. 4. Magnetization decay curves for residues S13 (upper panel) and V27 (bottom panel). Experimental data are shown with circles, while continuous lines represent fitting results. Blue and red color represent data related to the protonated sample and the deuterated sample, respectively. Data obtained on the protonated sample and the deuterated sample are normalized independently. (For interpretation of the references to color in this figure legend, the reader is referred to the web version of this article.)

the protonated sample. Residues in the termini show less T_1 difference, mainly because of their very short T_1 times, which are not long enough for chemical exchange. The significant difference in T_1 values gives the perfect opportunity to extract H/D substitution rates (see Fig. 3).

The evolution of ^{15}N magnetization under relaxation and chemical exchange in the deuterated sample is described by the Bloch-McConnell equations [15,47,48]:

$$\frac{d}{dt}\begin{pmatrix} N_Z^H(\Delta T+\delta t) \\ N_Z^D(\Delta T+\delta t)\end{pmatrix} = \begin{pmatrix} -R_1^{NH}-P_D\cdot k_{HD} & P_H\cdot k_{DH} \\ P_D\cdot k_{HD} & -R_1^{ND}-P_H\cdot k_{DH}\end{pmatrix}\begin{pmatrix} N_Z^H(\Delta T+\delta t) \\ N_Z^D(\Delta T+\delta t)\end{pmatrix} \quad (1)$$

where time-dependent magnetization of protonated and deuterated nitrogens is denoted by N_Z^H and N_Z^D, respectively. The proton and deuterium solvent ratios P_H and P_D are defined by the sample preparation protocol. The hydrogen-deuterium substitution rate k_{HD} relates to the inverse process by: $k_{DH} = k_{HD}/1.1$ [49]. Longitudinal relaxation rate of proton- and deuterium-bound nitrogens is given by R_1^{NH} and R_1^{DH}, respectively. In the pulse sequence (Fig. 1B), hydrogen exchange takes place not only during mixing time ΔT but also during a number of small delays, whose sum is denoted by δt. In the fully protonated sample, the deuterium fraction is zero and the system of equations (1) is reduced to a single equation that describes mono-exponential decay of ^{15}N magnetization. We performed a joint numerical analysis of the experimental data from the protonated and deuterated samples. All data points were treated equally in the least squares numerical fit, which was performed simultaneously on both data sets, employing an in-built optimization routine in MATLAB. The final system consisted of three coupled differential equations: one described evolution in the protonated sample, while two equations were necessary to describe dynamics in the deuterated sample. Initial N_Z^D magnetization was set to zero. In this case, the experimental data can be fitted with 5 parameters: exchange rate k_{HD}, R_1^{NH}, R_1^{ND} and initial magnetization N_Z^H in each experimental series. We limited the ratio of R_1^{ND}/R_1^{NH} to a quite broad interval between 0.05 and 5.0. Variations within this range have almost no effect on k_{HD} values, which was verified by additional fitting using different fixed R_1^{ND}/R_1^{NH} ratios.

Fitting results are illustrated for serine-13 and valine-27 in Fig. 4. Despite very long real T_1, no chemical exchange was observed for serine-13, as one can see from the upper panel. Valine-27 clearly shows faster ^{15}N magnetization decay in the deuterated sample, which is caused by H/D exchange.

Fig. 5 summarizes the extracted exchange rates as a function of residue position. All exchange rates are very slow and below 0.06 s^{-1}.

The slow timescale accessible by this method is limited by the longitudinal relaxation rates of the nitrogens. If the ^{15}N longitudinal relaxation times are significantly shorter than the H/D exchange time, the latter cannot be reliably quantified. Previous studies by Chevelkov et al. [50] compared ^{15}N T_1 rates in protonated and deuterated α-spectrin SH3 domain samples obtained on a 600 MHz spectrometer by carbon- and proton-detected experiments, respectively. The differences in relaxation times were too small to reliably quantify H/D exchange. Later, Reif and coworkers [33] obtained H/D exchange rates for just three amide sites in the α-spectrin SH3 domain. All of these experiments demonstrated that H/D exchange is hardly accessible even for a small solid state model protein, mainly because ^{15}N T_1 is not long enough to allow hydrogen-deuterium substitution. Due to this limitation, we conducted experiments at a high external magnetic field (800 MHz), in order to maximize ^{15}N T_1 [46,50]. The observed exchange rates are several times slower than the rates previously obtained in SH3 [33], which clearly demonstrates the power of the Relax-EXSY approach. The obtained results demonstrate that H/D exchange in a solid state phase can be high enough to distort ^{15}N T_1 measured in samples with a considerable fraction of D_2O in buffer.

4. Conclusion

We demonstrated that hydrogen-deuterium exchange of amide protons in solid state proteins can be reliably measured by MAS NMR at equilibrium conditions. The approach requires proton detection, which broadens the applicability of this technique in solid state NMR. In general, the method demonstrates the very high sensitivity achieved by a set of simple and straightforward experiments. The method applied to the PrgI T3SS needle protein yielded exchange rates for 40 residues and can be efficiently used to study the chemical exchange process in many biomolecules.

Acknowledgments

We thank Brigitta Angerstein for expert technical assistance. We thank Eve Ousby for valuable discussions. This work was supported by the Leibniz-Forschungsinstitut für Molekulare Phar-

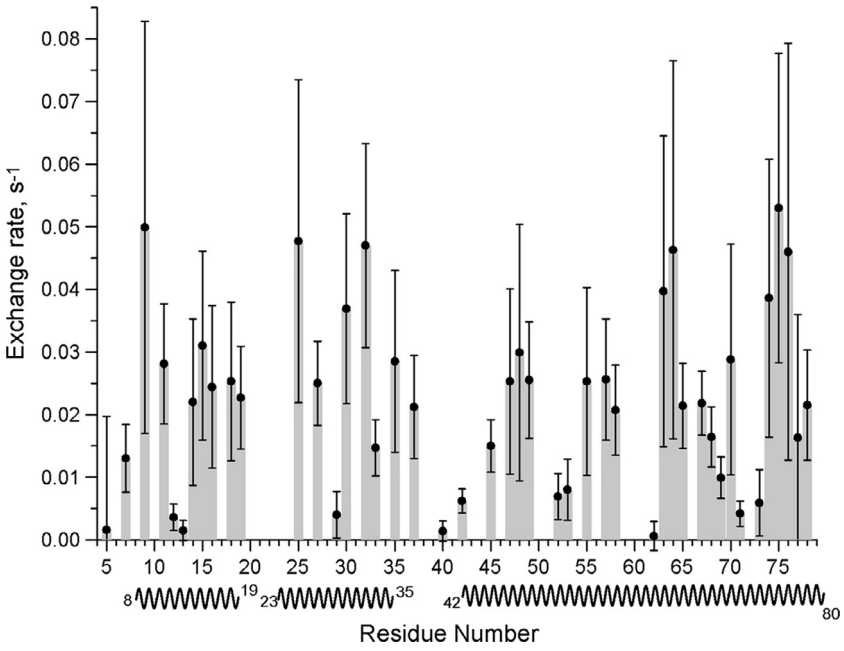

Fig. 5. Exchange rate constant k_{HD} as a function of amino acid sequence of Prgl. See Supporting Information (Table 1) for all numeric values.

makologie, the Max Planck Society, the European Research Council (ERC Starting Grant to A.L.), the German Research Foundation (Deutsche Forschungsgemeinschaft; Emmy Noether Fellowship to A.L.).

Appendix A. Supplementary material

Supplementary data associated with this article can be found, in the online version, at https://doi.org/10.1016/j.jmr.2017.08.012.

References

[1] A. Hvidt, K. Linderstromlang, Exchange of hydrogen atoms in insulin with deuterium atoms in aqueous solutions, Biochim. Biophys. Acta 14 (1954) 574–575.
[2] C.E. Dempsey, Hydrogen exchange in peptides and proteins using NMR-spectroscopy, Prog. Nucl. Magn. Reson. Spectrosc. 39 (2001) 135–170.
[3] G. Wagner, K. Wuthrich, Amide proton-exchange and surface conformation of the basic pancreatic trypsin-inhibitor in solution - studies with two-dimensional nuclear magnetic-resonance, J. Mol. Biol. 160 (1982) 343–361.
[4] H. Roder, G.A. Elove, S.W. Englander, Structural characterization of folding intermediates in cytochrome-c by h-exchange labeling and proton NMR, Nature 335 (1988) 700–704.
[5] M. Gal, P. Schanda, B. Brutscher, L. Frydman, UltraSOFAST HMQC NMR and the repetitive acquisition of 2D protein spectra at Hz rates, J. Am. Chem. Soc. 129 (2007) 1372–1377.
[6] C.M. Dobson, L.Y. Lian, C. Redfield, K.D. Topping, Measurement of hydrogen-exchange rates using 2D NMR-spectroscopy, J. Magn. Reson. 69 (1986) 201–209.
[7] G. Otting, E. Liepinsh, K. Wuthrich, Protein hydration in aqueous-solution, Science 254 (1991) 974–980.
[8] S. Spera, M. Ikura, A. Bax, Measurement of the exchange rates of rapidly exchanging amide protons: application to the study of calmodulin and its complex with a myosin light chain kinase fragment, J. Biomol. NMR 1 (1991) 155–165.
[9] R.W. Kriwacki, R.B. Hill, J.M. Flanagan, J.P. Caradonna, J.H. Prestegard, New NMR methods for the characterization of bound waters in macromolecules, J. Am. Chem. Soc. 115 (1993) 8907–8911.
[10] S. Grzesiek, A. Bax, The importance of not saturating H2O in protein NMR - application to sensitivity enhancement and NOE measurements, J. Am. Chem. Soc. 115 (1993) 12593–12594.
[11] S. Mori, C. Abeygunawardana, P.C.M. van Zijl, J.M. Berg, Water exchange filter with improved sensitivity (WEX II) to study solvent-exchangeable protons. Application to the consensus zinc finger peptide CP-I, J. Magn. Reson. B 110 (1996) 96–101.
[12] J. Zhou, P.C.M. van Zijl, Chemical exchange saturation transfer imaging and spectroscopy, Prog. Nucl. Magn. Reson. Spectrosc. 48 (2006) 109–136.
[13] V. Chevelkov, Y. Xue, D.K. Rao, J.D. Forman-Kay, N.R. Skrynnikov, N-15(H/D)-SOLEXSY experiment for accurate measurement of amide solvent exchange rates: application to denatured drkN SH3, J. Biomol. NMR 46 (2010) 227–244.
[14] T.L. Hwang, P.C.M. van Zijl, S. Mori, Accurate quantitation of water-amide proton exchange rates using the phase-modulated CLEAN chemical EXchange (CLEANEX-PM) approach with a Fast-HSQC (FHSQC) detection scheme, J. Biomol. NMR 11 (1998) 221–226.
[15] J. Lopez, P. Ahuja, I. Landrieu, F.X. Cantrelle, I. Huvent, G. Lippens, H/D exchange of a N-15 labelled Tau fragment as measured by a simple Relax-EXSY experiment, J. Magn. Reson. 249 (2014) 32–37.
[16] W. Gallagher, F. Tao, C. Woodward, Comparison of hydrogen-exchange rates for bovine pancreatic trypsin-inhibitor in crystals and in solution, Biochemistry 31 (1992) 4673–4680.
[17] N.A. Whittemore, R. Mishra, I. Kheterpal, A.D. Williams, R. Wetzel, E.H. Serpersu, Hydrogen-deuterium (H/D) exchange mapping of Aβ(1–40) amyloid fibril secondary structure using nuclear magnetic resonance spectroscopy, Biochemistry 44 (2005) 4434–4441.
[18] M. Hoshino, H. Katou, K.I. Yamaguchi, Y. Goto, Dimethylsulfoxide-quenched hydrogen/deuterium exchange method to study amyloid fibril structure, Biochim. Biophys. Acta 1768 (2007) 1886–1899.
[19] S.L. Wang, L.C. Shi, I. Kawamura, L.S. Brown, V. Ladizhansky, Site-specific solid-state NMR detection of hydrogen-deuterium exchange reveals conformational changes in a 7-helical transmembrane protein, Biophys. J. 101 (2011) L23–L25.
[20] J. Medeiros-Silva, S. Jekhmane, M. Baldus, M. Weingarth, Hydrogen bond strength in membrane proteins probed by time-resolved ^{1}H-detected solid-state NMR and MD simulations, Solid State Nucl. Magn. Reson. (2017).
[21] K. Grohe, K.T. Movellan, S.K. Vasa, K. Giller, S. Becker, R. Linser, Non-equilibrium hydrogen exchange for determination of H-bond strength and water accessibility in solid proteins, J Biomol NMR (2017) 1–11.
[22] A. Lesage, A. Bockmann, Water-protein interactions in microcrystalline Crh measured by ^{1}H-^{13}C solid-state NMR spectroscopy, J. Am. Chem. Soc. 125 (2003) 13336–13337.
[23] V. Chevelkov, K. Faelber, A. Diehl, U. Heinemann, H. Oschkinat, B. Reif, Detection of Water Molecules in a polycrystalline sample of a chicken a-spectrin SH3 domain, J. Biomol. NMR 31 (2005) 295–310.
[24] A. Lesage, C. Gardiennet, A. Loquet, R. Verel, G. Pintacuda, L. Emsley, B.H. Meier, A. Bockmann, Polarization transfer over the water-protein interface in solids, Angew. Chem. Int. Ed. 47 (2008) 5851–5854.
[25] I.V. Sergeyev, S. Bahri, L.A. Day, A.E. McDermott, Pf1 bacteriophage hydration by magic angle spinning solid-state NMR, J. Chem. Phys. 141 (2014) 13.
[26] J.K. Williams, M. Hong, Probing membrane protein structure using water polarization transfer solid-state NMR, J. Magn. Reson. 247 (2014) 118–127.
[27] A. Boeckmann, C. Gardiennet, R. Verel, A. Hunkeler, A. Loquet, G. Pintacuda, L. Emsley, B.H. Meier, A. Lesage, Characterization of different water pools in solid-state NMR protein samples, J. Biomol. NMR 45 (2009) 319–327.
[28] H. Van Melckebeke, P. Schanda, J. Gath, C. Wasmer, R. Verel, A. Lange, B.H. Meier, A. Bockmann, Probing water accessibility in HET-s(218–289) amyloid fibrils by solid-state NMR, J. Mol. Biol. 405 (2011) 765–772.
[29] M. Weingarth, E.A.W. van der Cruijsen, J. Ostmeyer, S. Lievestro, B. Roux, M. Baldus, Quantitative analysis of the water occupancy around the selectivity

filter of a K^+ channel in different gating modes, J. Am. Chem. Soc. 136 (2014) 2000–2007.
[30] T. Wang, H. Jo, W.F. DeGrado, M. Hong, Water distribution, dynamics, and interactions with Alzheimer's β-amyloid fibrils investigated by solid-state NMR, J. Am. Chem. Soc. 139 (2017) 6242–6252.
[31] D.H. Zhou, C.M. Rienstra, High-performance solvent suppression for proton detected solid-state NMR, J. Magn. Reson. 192 (2008) 167–172.
[32] V. Chevelkov, S.Q. Xiang, K. Giller, S. Becker, A. Lange, B. Reif, Perspectives for sensitivity enhancement in proton-detected solid-state NMR of highly deuterated proteins by preserving water magnetization, J. Biomol. NMR 61 (2015) 151–160.
[33] J.M. Lopez del Amo, U. Fink, B. Reif, Quantification of protein backbone hydrogen-deuterium exchange rates by solid state NMR spectroscopy, J. Biomol. NMR 48 (2010) 203–212.
[34] A. Loquet, G. Lv, K. Giller, S. Becker, A. Lange, ^{13}C spin dilution for simplified and complete solid-state NMR resonance assignment of insoluble biological assemblies, J. Am. Chem. Soc. 133 (2011) 4722–4725.
[35] A. Loquet, N.G. Sgourakis, R. Gupta, K. Giller, D. Riedel, C. Goosmann, C. Griesinger, M. Kolbe, D. Baker, S. Becker, A. Lange, Atomic model of the type III secretion system needle, Nature 486 (2012) 276–279.
[36] V. Chevelkov, B. Habenstein, A. Loquet, K. Giller, S. Becker, A. Lange, Proton-detected MAS NMR experiments based on dipolar transfers for backbone assignment of highly deuterated proteins, J. Magn. Reson. 242 (2014) 180–188.
[37] V. Chevelkov, K. Rehbein, A. Diehl, B. Reif, Ultrahigh resolution in proton solid-state NMR spectroscopy at high levels of deuteration, Angew. Chem. Int. Ed. 45 (2006) 3878–3881.
[38] N. Giraud, A. Bockmann, A. Lesage, F. Penin, M. Blackledge, L. Emsley, Site-specific backbone dynamics from a crystalline protein by solid-state NMR spectroscopy, J. Am. Chem. Soc. 126 (2004) 11422–11423.
[39] A. Pines, J.S. Waugh, M.G. Gibby, Proton-enhanced nuclear induction spectroscopy - method for high-resolution NMR of dilute spins in solids, J. Chem. Phys. 56 (1972) 1776–1777.
[40] M. Baldus, A.T. Petkova, J. Herzfeld, R.G. Griffin, Cross polarization in the tilted frame: assignment and spectral simplification in heteronuclear spin systems, Mol. Phys. 95 (1998) 1197–1207.
[41] B.M. Fung, A.K. Khitrin, K. Ermolaev, An improved broadband decoupling sequence for liquid crystals and solids, J. Magn. Reson. 142 (2000) 97–101.
[42] A.J. Shaka, J. Keeler, T. Frenkiel, R. Freeman, An improved sequence for broad-band decoupling - WALTZ-16, J. Magn. Reson. 52 (1983) 335–338.
[43] V. Chevelkov, A.V. Zhuravleva, Y. Xue, B. Reif, N.R. Skrynnikov, Combined analysis of ^{15}N relaxation data from solid- and solution-state NMR spectroscopy, J. Am. Chem. Soc. 129 (2007) 12594–12595.
[44] E.K. Paulson, C.R. Morcombe, V. Gaponenko, B. Dancheck, R.A. Byrd, K.W. Zilm, Sensitive high resolution inverse detection NMR spectroscopy of proteins in the solid state, J. Am. Chem. Soc. 125 (2003) 15831–15836.
[45] P. Fricke, D. Mance, V. Chevelkov, K. Giller, S. Becker, M. Baldus, A. Lange, High resolution observed in 800 MHz DNP spectra of extremely rigid type III secretion needles, J. Biomol. NMR 1–6 (2016).
[46] P. Schanda, B.H. Meier, M. Ernst, Quantitative analysis of protein backbone dynamics in microcrystalline ubiquitin by solid-state NMR spectroscopy, J. Am. Chem. Soc. 132 (2010) 15957–15967.
[47] H.M. McConnell, Reaction rates by nuclear magnetic resonance, J. Chem. Phys. 28 (1958) 430–431.
[48] J. Jeener, B.H. Meier, P. Bachmann, R.R. Ernst, Investigation of exchange processes by 2-dimensional NMR-spectroscopy, J. Chem. Phys. 71 (1979) 4546–4553.
[49] A.C. LiWang, A. Bax, Equilibrium protium/deuterium fractionation of backbone amides in U-^{13}C-^{15}N labeled human ubiquitin by triple resonance NMR, J. Am. Chem. Soc. 118 (1996) 12864–12865.
[50] V. Chevelkov, A. Diehl, B. Reif, Measurement of ^{15}N-T_1 relaxation rates in a perdeuterated protein by magic angle spinning solid-state nuclear magnetic resonance spectroscopy, J. Chem. Phys. 128 (2008).